Chemical Science

ROYAL SOCIETY OF CHEMISTRY

EDGE ARTICLE

View Article Online
View Journal | View Issue

Check for updates

Cite this: *Chem. Sci.*, 2025, **16**, 12594

All publication charges for this article have been paid for by the Royal Society of Chemistry

Received 12th April 2025
Accepted 4th June 2025

DOI: 10.1039/d5sc02711j

rsc.li/chemical-science

Rh-catalyzed enantioselective hydrosilylation of unactivated alkenes†

Yichen Wu,‡*[a] Hao-Yang Qian,‡[a] Heng Zhang,‡[b] Jian-Ye Zou,[a] Qing-Yan Wu,[a] Xiao-Xue Nie,[a] Long Zheng,[a] Qian Peng *[b] and Peng Wang *[acd]

Here, we report a highly efficient rhodium-catalysed enantioselective hydrosilylation of unactivated alkenes, achieving excellent regioselectivity and high enantioselectivity. The use of a commercially available chiral ferrocene-based phosphine–oxazoline ligand was crucial in achieving excellent chiral induction and high reactivity with undirected unactiviated alkenes, delivering Si-stereogenic monohydrosilanes in high yields and excellent enantioselectivities. This protocol represents a robust, scalable method for the enantioselective synthesis of Si-stereogenic monohydrosilanes, featuring a low catalyst loading, a broad substrate scope and exceptional functional group and heterocycle tolerance. Moreover, the late-stage functionalization of complex motifs opens a new avenue for incorporating chiral silicon motifs into pharmaceuticals and bioactive compounds.

Introduction

Organosilanes are a class of versatile compounds and have already been utilized as synthetic linchpins, catalysts, adhesion promoters, sensors, *etc.* in both fundamental research and industrial processes.[1] Among those valuable organosilanes, Si-stereogenic organosilanes are emerging as a particularly compelling class of architectures due to their unique potential in synthetic chemistry, advanced materials, and pharmaceutical design (Scheme 1a).[2] Their stereochemical complexity opens up new possibilities in areas such as mechanistic study, chiral recognition, catalysts, CPL materials, and drug development. For example, a cyclic monohydrosilane has been applied as the mechanistic probe by Oestreich and co-workers.[3] Furthermore, recent advances in chiral ligand design,[4] such as spirosilacycle-based chiral ligands, demonstrate the growing role of silicon stereochemistry in asymmetric catalysis. Despite the growing demand in fields like medicinal chemistry and materials science, expanding the repertoire of Si-stereogenic organosilanes remains an unmet challenge.[5] Currently, existing strategies, including hydrosilylation,[4a,6–8] dehydrogenative silylation,[9] carbene insertion[10] and cross-coupling,[11] *etc.* have made strides toward novel Si-stereogenic architectures. However, the development of robust and scalable methods for accessing these highly coveted structures remains a critical objective.

Transition-metal-catalyzed enantioselective hydrosilylation of alkenes offers one of the most direct and efficient ways for constructing organosilane frameworks with 100% atom economy.[12] While numerous studies have demonstrated for the access of carbon-stereogenic organosilanes, which serve as key intermediates for the preparation of diverse chiral molecules, the preparation of silicon-stereogenic organosilanes *via* the transition-metal-catalysed hydrosilylation of alkenes[6a–h] remains far less explored. This is probably due to inherent challenges in controlling stereochemistry around silicon, as the longer Si–H bond and the large atomic radius of silicon introduce a highly flexible transition state in the transition-metal catalysed hydrosilylation event. To data, access to Si-stereogenic organosilanes *via* transition metal-catalysed hydrosilylation of alkenes has been limited to intramolecular reactions[6a,b,e,h] or intermolecular processes involving highly reactive substrates, such as 1,4-dienes,[6g] enynes[6f] and methylenecyclopropanes (MCPs).[6i,j] The intermolecular hydrosilylation of unactivated alkenes for the construction of Si-stereogenic compounds remains a big challenge due to the low reactivity of unactivated alkenes and the difficulties in controlling the

[a]*State Key Laboratory of Organometallic Chemistry and Shanghai-Hong Kong Joint Laboratory in Chemical Synthesis, Shanghai Institute of Organic Chemistry, University of Chinese Academy of Sciences, CAS 345 Lingling Road, Shanghai, 200032, P. R. China. E-mail: ywu@sioc.ac.cn; pengwang@sioc.ac.cn*

[b]*State Key Laboratory of Elemento-Organic Chemistry, Frontiers Science Center for New Organic Matter, Tianjin Key Laboratory of Biosensing and Molecular Recognition, College of Chemistry, Nankai University, Tianjin, 300071, P. R. China. E-mail: qpeng@nankai.edu.cn*

[c]*School of Chemistry and Materials Science, Hangzhou Institute for Advanced Study, University of Chinese Academy of Sciences, 1 Sub-lane Xiangshan, Hangzhou, 310024, P. R. China*

[d]*College of Material Chemistry and Chemical Engineering, Key Laboratory of Organosilicon Chemistry, and Material Technology of Ministry of Education, Hangzhou Normal University, Hangzhou, 311121, P. R. China*

† Electronic supplementary information (ESI) available. CCDC 2393477. For ESI and crystallographic data in CIF or other electronic format see DOI: https://doi.org/10.1039/d5sc02711j

‡ Those authors contributed equally.

Open Access Article. Published on 05 June 2025. Downloaded on 2/8/2026 8:22:49 PM. This article is licensed under a Creative Commons Attribution-NonCommercial 3.0 Unported Licence.

© 2025 The Author(s). Published by the Royal Society of Chemistry

Open Access Article. Published on 05 June 2025. Downloaded on 2/8/2026 8:22:49 PM. This article is licensed under a Creative Commons Attribution-NonCommercial 3.0 Unported Licence.

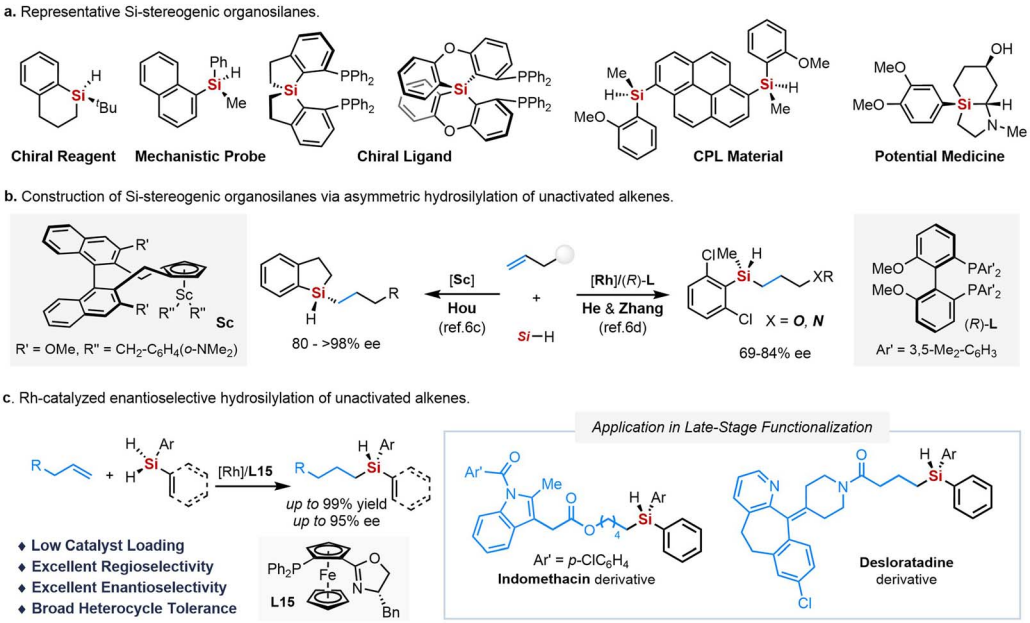

Scheme 1 Synopsis for Rh-catalysed enantioselective hydrosilylation.

regio- and stereo-selectivities. In this context, the Hou group has reported an elegant example of intermolecular hydrosilylation of unactivated alkenes employed an air-sensitive and pre-prepared chiral half-sandwich scandium catalyst at high temperature (left, Scheme 1b).[6c] More recently, He, Zhang and co-workers have mentioned a Rh-catalysed intermolecular hydrosilylation of unactivated alkenes could only be realized with moderated chiral induction (up to 84% ee) employing unactivated alkenes bearing heteroatom-coordinating groups (right, Scheme 1b).[6d] During the submission of this manuscript, the Xu group reported a Cu-catalysed asymmetric hydrosilylation of terminal alkenes.[13] Herein, we report a rhodium-catalysed enantioselective hydrosilylation of unactivated alkenes, enabling the construction of Si-stereogenic monohydrosilanes with remarkable regioselectivity and enantioselectivity. Crucially, this reaction features very mild conditions, a broad substrate scope, excellent functional group and heterocycle tolerance. The combination of rhodium catalyst and the commercially available ferrocene-based phosphine–oxazoline ligand (phosferrox) is crucial for the high reactivity with undirected unactivated alkenes and chiral induction, resulting in the Si-stereogenic monohydrosilanes in excellent regioselectivities and high enantioselectivities. The catalyst loading could be lower down to 0.5 mol% without a decrease of efficiency and chiral induction, demonstrating this protocol a robust, scalable method for the enantioselective synthesis of Si-stereogenic monohydrosilanes, which could convert to other functional Si-stereogenic organosilanes in a stereospecific manner. More importantly, this strategy not only overcomes the limitations previously associated with silicon stereochemistry *via* intermolecular hydrosilylation of alkenes, but also opens new avenues for the incorporation of chiral silicon motifs into complex molecules, particularly in the realm of pharmaceuticals, where late-stage functionalization is of paramount importance. Mechanistic and computational studies indicate the reaction might undergo a Chalk–Harrod mechanism, and the C–Si reductive elimination might be both rate- and enantio-determining step (Scheme 1c).

Results and discussion

We initiated our investigation by using dihydrosilane **1a** and 4-phenyl-1-butene (**2**) as the model substrates, and employing $[Rh(cod)Cl]_2$ as the catalyst. Although the Rh-catalysed enantioselective intermolecular hydrosilylation of unactivated alkenes without a coordination group remains challenge in the literature,[6d] we were glad to find that this hydrosilylation gave the desired linear selective hydrosilylated product in high yield (80% yield) and excellent regioselectivity, albeit with an unsatisfying enantioselectivity (23% ee) when (*R*)-BINAP was added as the ligand under very mild reaction conditions (30 °C in methyl *tert*-butyl ether). Recognizing the critical role of the ligand in transition-metal catalysed asymmetric reactions, we first examined the influence of various ligands on this hydrosilylation reaction (Scheme 2a). Since phosphine ligands are commonly applied in Rh-catalysed asymmetric hydrosilylation, we evaluated a range of phosphine ligands with axial (**L1–L3**), central (**L4–L8**), or planar (**L9**) chirality. However, these ligands yielded the target product **3a** with low enantioselectivities (<26% ee). Interestingly, a chiral phosphine–oxazoline ligand with a ferrocenyl backbone, (*S*,*Rp*)-^{i}Pr-phosferrox (**L11**), showed promising chiral induction (46% ee), with an even higher ee value observed with the (*R*)-^{i}Pr variant (**L12**, −59% ee). Following this lead, the steric influence of phosferrox ligands on this reaction was further evaluated, finding that the optimal yield and enantioselectivity (52%, 74% ee) were achieved using

Open Access Article. Published on 05 June 2025. Downloaded on 2/8/2026 8:22:49 PM.
This article is licensed under a Creative Commons Attribution-NonCommercial 3.0 Unported Licence.

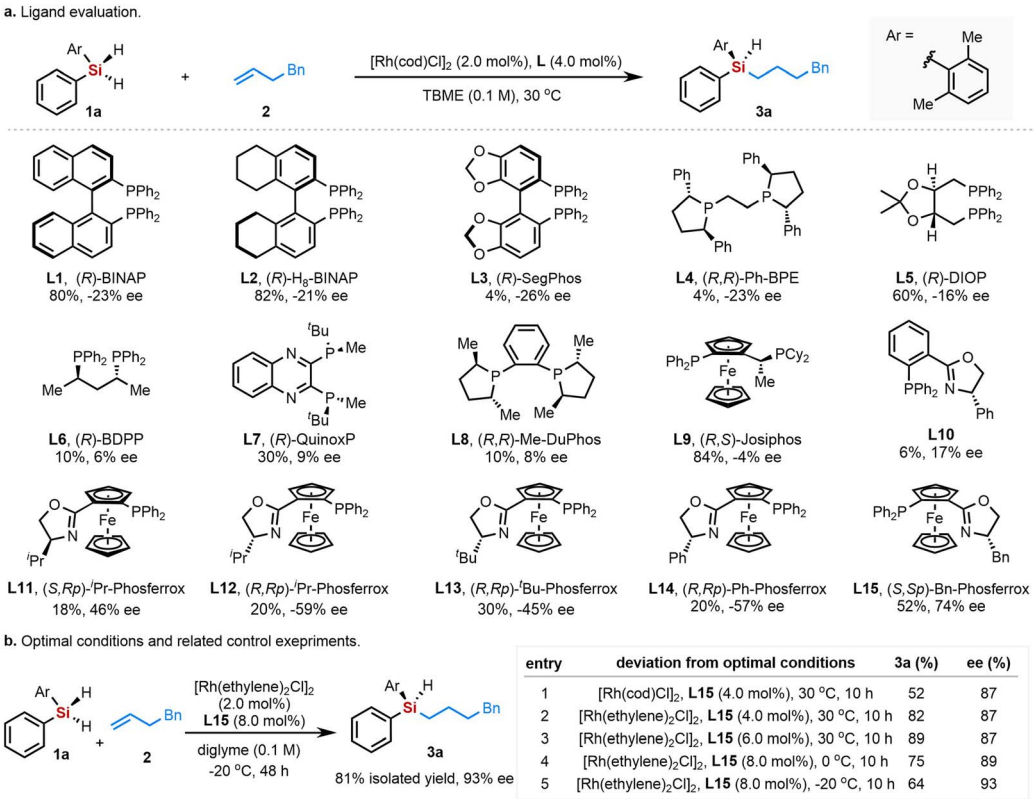

entry	deviation from optimal conditions	3a (%)	ee (%)
1	[Rh(cod)Cl]$_2$, **L15** (4.0 mol%), 30 °C, 10 h	52	87
2	[Rh(ethylene)$_2$Cl]$_2$, **L15** (4.0 mol%), 30 °C, 10 h	82	87
3	[Rh(ethylene)$_2$Cl]$_2$, **L15** (6.0 mol%), 30 °C, 10 h	89	87
4	[Rh(ethylene)$_2$Cl]$_2$, **L15** (8.0 mol%), 0 °C, 10 h	75	89
5	[Rh(ethylene)$_2$Cl]$_2$, **L15** (8.0 mol%), -20 °C, 10 h	64	93

Scheme 2 Ligand evaluation for enantioselective Rh-catalyzed hydrosilylation.

(*S*,*Sp*)-Bn-phosferrox (**L15**) which has been employed in Rh-catalyzed hydrosilylation of carbonyl compounds recently.[8e] The sterically hindered (*R*,*Rp*)-^{t}Bu-phosferrox (**L13**) and (*R*,*Rp*)-Ph-phosferrox (**L14**) afforded comparable reactivity with **L12**. After systematically screening the influence of solvents, diglyme proved to be the optimal one, providing **3a** in the highest enantioselectivity (52% yield, 87% ee). Replacement of [Rh(cod)Cl]$_2$ with [Rh(ethylene)$_2$Cl]$_2$ further increased the yield to 82% (entry 2, Scheme 2b). After systematically evaluation of other reaction parameters, the efficiency and enantioselectivity of this reaction were further improved to 81% isolated yield with 93% ee by conducting this reaction at −20 °C in diglyme in the presence of [Rh(ethylene)$_2$Cl]$_2$ (2.0 mol%) and (*S*,*Sp*)-Bn-phosferrox **L15** (8.0 mol%). The absolution configuration of the hydrosilylated product was determined by X-ray crystallographic analysis of **5j**,[14] revealing an (*S*)-configuration (Scheme 4).

With the optimized conditions established, we explored the substrate scope of this reaction with various dihydrosilanes (Scheme 3). A series of unsymmetric dihydrodiarylsilanes, bearing both electron-rich and electron-deficient aryl groups, proceeded smoothly to deliver the desired silicon-stereogenic monohydrosilanes in high yields and excellent enantioselectivities. A broad spectrum of functionalities, including alkyl (**1b–d**), methoxy (**1f**), trimethylsilyl (TMS, **1e**), fluoro (**1i**, **1m**), chloro (**1j**, **1n**, **1t**), trifluoromethyl (**1k**, **1o**) *etc.*, were well compatible in this protocol, demonstrating the versatility of this protocol. The substituents at *para*- (**1b–k**) and *meta*- (**1l–o**) positions normally exhibited similar levels of chiral induction. Furthermore, dihydrosilanes with 2-naphthyl group (**1p**) and piperonyl group (**1q**) were both well tolerated in this asymmetric hydrosilylation, offering the corresponding products with an enantioselectivities of up to 94% ee. It is worth noting that alkenyl substituted dihydrosilane **1r** proved to be a suitable substrate, providing the corresponding product **3r** in 64% yield and 92% ee. However, the dihydrosilane bearing a styrenyl group (**1s**) resulted in lower enantioselectivity, likely due to the decreased steric hindrance around the silicon center.

Next, the generality of unactivated alkenes for this newly developed protocol was explored. As shown in Scheme 4, a wide variety of unactivated alkenes with diverse functional groups were smoothly converted to the corresponding hydrosilylated products **5** with moderate to high yields with excellent enantioselectivities. The reaction features excellent functional group tolerance, accommodating methoxy (**4b**), trifluoromethyl (**4c**), chloro (**4e**), bromo (**4f**), ester (**4g**), silylether (**4h**), native secondary amine (**4i**), and amide groups (**4j–k**). Those substrates gave the hydrosilylated products in up to 98% yield with enantioselectivities ranging from 81–95% ee. The reaction with alkene containing ferrocene (**4l**) proceeded smoothly to offer the target product in 81% yield and 92% ee. Notably, the protocol demonstrated exceptional tolerance for substrates containing strongly coordinating heterocycles, such as pyridine (**4r**) and quinoline (**4s**), which are traditionally challenging in transition-metal catalysed reactions due to their strong coordination to metal centers. Despite these challenges, the reaction

© 2025 The Author(s). Published by the Royal Society of Chemistry

Open Access Article. Published on 05 June 2025. Downloaded on 2/8/2026 8:22:49 PM.
This article is licensed under a Creative Commons Attribution-NonCommercial 3.0 Unported Licence.

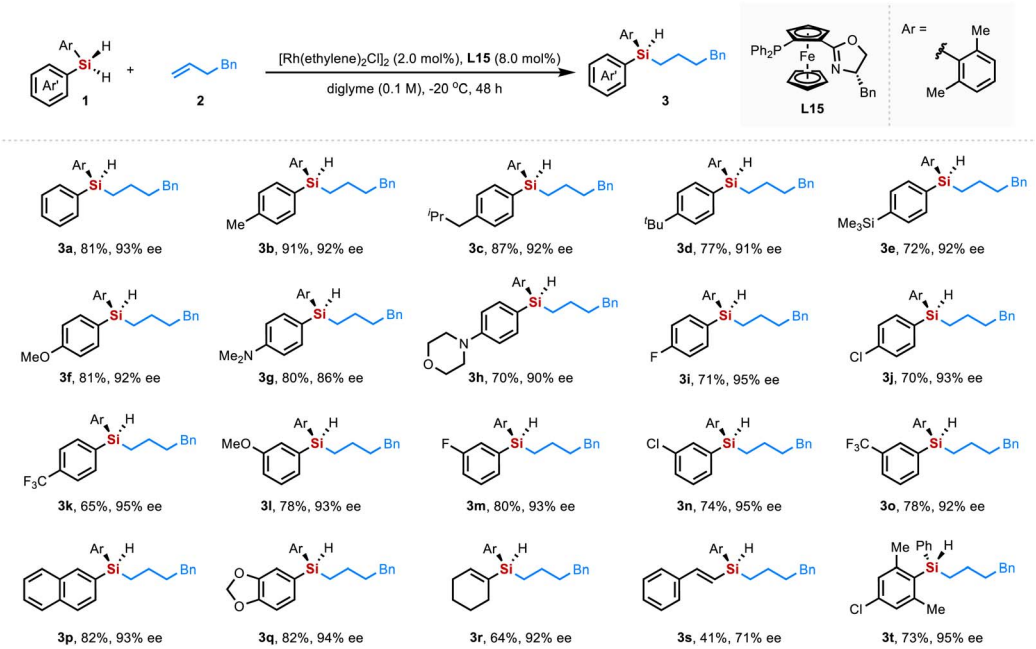

Scheme 3 Scope of dihydrosilanes[a,b]. [a]Reaction conditions: **1** (0.2 mmol), **2** (31.8 mg, 0.24 mmol), $[Rh(ethylene)_2Cl]_2$ (1.6 mg, 2.0 mol%), **L15** (8.4 mg, 8.0 mol%), diglyme (2.0 mL), −20 °C, 48 h, N_2. [b]Isolated yield; the ee value was determined by chiral HPLC analysis.

proceeded smoothly, delivering the desired products in high yields (up to 97%) and with excellent enantioselectivities (up to 95% ee). This robustness underscores the versatility of the catalytic system and its ability to handle coordination-prone substrates without compromising reactivity or stereoselectivity. Additionally, other heterocycle-containing alkenes, including benzothiophene (**4m**), carbazole (**4n**), phenothiazine (**4o**), furan (**4p**), and thiophene (**4q**), were well tolerated,

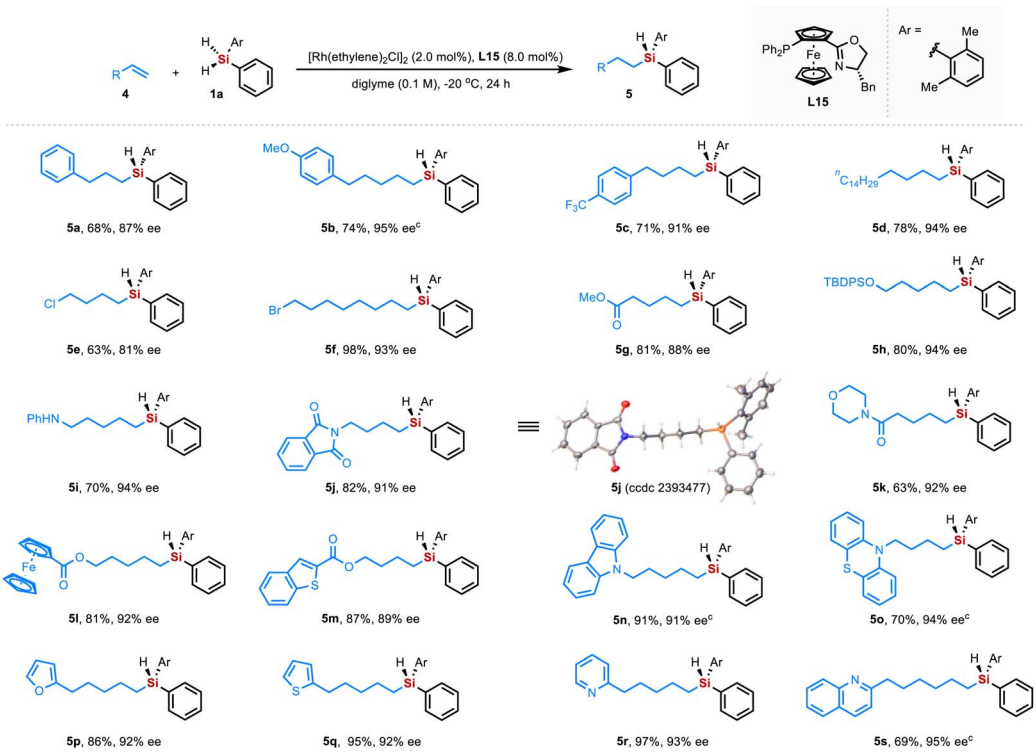

Scheme 4 Scope of unactive alkenes[a,b]. [a]Reaction conditions: **1a** (42.5 mg, 0.2 mmol), **4** (0.24 mmol), $[Rh(ethylene)_2Cl]_2$ (1.6 mg, 2.0 mol%), **L15** (8.4 mg, 8.0 mol%), diglyme (2.0 mL), −20 °C, 24 h, N_2. [b]Isolated yield; the ee value was determined by chiral HPLC analysis. [c]48 h.

Open Access Article. Published on 05 June 2025. Downloaded on 2/8/2026 8:22:49 PM.
This article is licensed under a Creative Commons Attribution-NonCommercial 3.0 Unported Licence.

affording the desired products in yields ranging from 70–95% and up to 94% ee.

To underscore the synthetic utility of this newly developed protocol, a gram-scale reaction was first conducted. Notably, the catalyst loading could be reduced to 0.5 mol% without any diminish in enantioselectivity (93% ee, Scheme 5a). This result showcases the efficiency and scalability of the method, making it highly practical for larger-scale applications. Next, this protocol was applied to the late-stage functionalization of complex molecules (Scheme 5b). The drug derivative of probenecid (**6a**), containing a sulfonamide functional group, was tolerated, delivering the corresponding hydrosilylated product in a synthetically useful yield with excellent enantioselectivity (56% yield, 94% ee). Moreover, the versatility of this method was further demonstrated by the installation of silicon-stereogenic center on other drug derivatives, including indomethacin (**7b**), desloratadine (**7c**), isoxepac (**7d**) and atomoxetine (**7e**). In all cases, the insertion of the Si-stereogenic fragment proceeded smoothly, affording the target compounds with high efficiency and excellent chiral induction. The robust tolerance for heteroatoms and heterocycles underscores the potential of this protocol in pharmaceutical synthesis, particularly for late-stage functionalization and for the preparation of silicon-containing compounds. Additionally, the resulted silicon-stereogenic monohydrosilane could serve as versatile synthetic precursor for the construction of other silicon-stereogenic organosilanes *via* stereospecific transformations. Using optical **5j** as the model substrate, the derivatizations of optical **5j** were also performed (Scheme 5c). The chiral silanol **8** could be obtained with no loss in enantioselectivity using Pd/C as catalyst and water as hydroxyl source. Stereospecific formation of tetraorganosilane **9** *via* carbene insertion further highlighted the method's capacity for constructing complex silicon-stereogenic architectures. Moreover, **5j** could be converted to silyl ether **10** *via* the copper-catalyzed etherification, with only a slight decrease in enantioselectivity (91% ee *vs.* 93% ee).

The preliminary mechanistic studies were carried out to gain insight into this Rh-catalysed asymmetric hydrosilylation of unactivated alkenes (Scheme 6). Based on our previous work,[6e,h] where we demonstrated that Rh-catalysed hydrosilylation of alkenes with dihydrosilanes proceeds *via* a Chalk–Harrod mechanism involving Rh–H insertion, we hypothesized that this reaction might follow a similar pathway. To probe this, a deuterium-labeling experiment was performed using deuterated substrate **1a-D** and 4-phenyl-1-butene **2** under standard conditions (Scheme 6a). The deuterated hydrosilylated product **3a-D** was obtained in 72% yield, with the deuterium exclusively located at the β-position relative to the silicon atom. This observation might be elucidated by the rapid insertion of alkene in to Rh–H intermediate, followed by the reductive elimination. However, 12% of

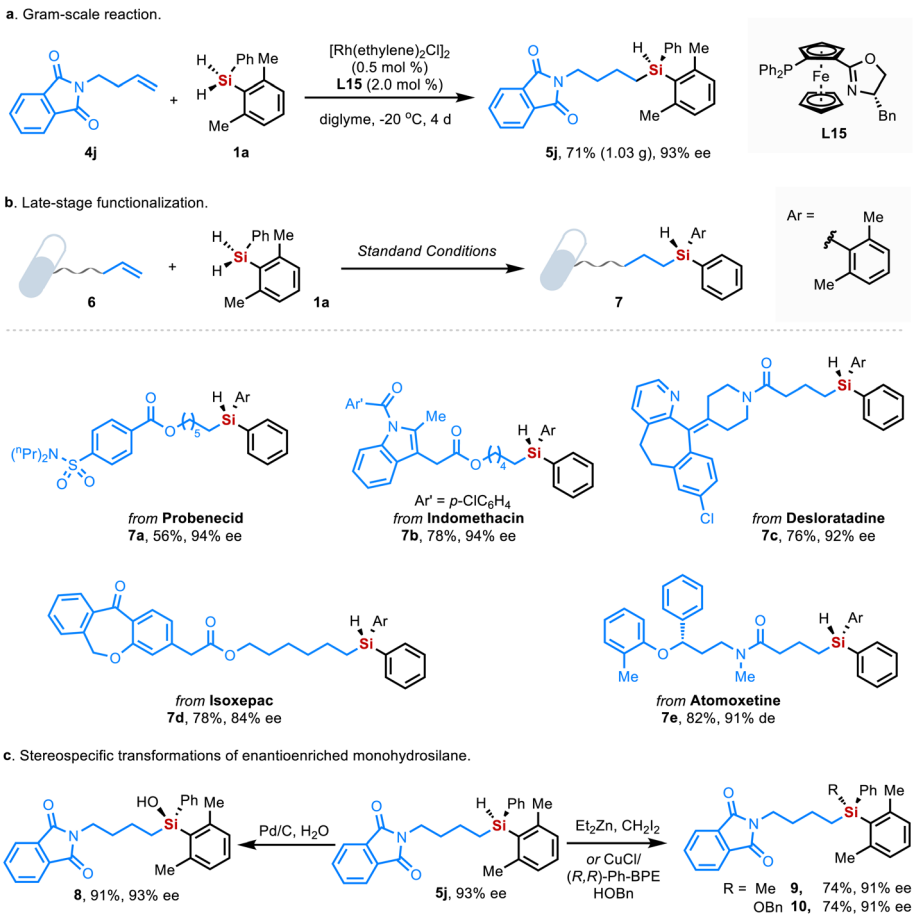

Scheme 5 Gram-scale reaction and synthetic applications.

© 2025 The Author(s). Published by the Royal Society of Chemistry

Open Access Article. Published on 05 June 2025. Downloaded on 2/8/2026 8:22:49 PM. This article is licensed under a Creative Commons Attribution-NonCommercial 3.0 Unported Licence.

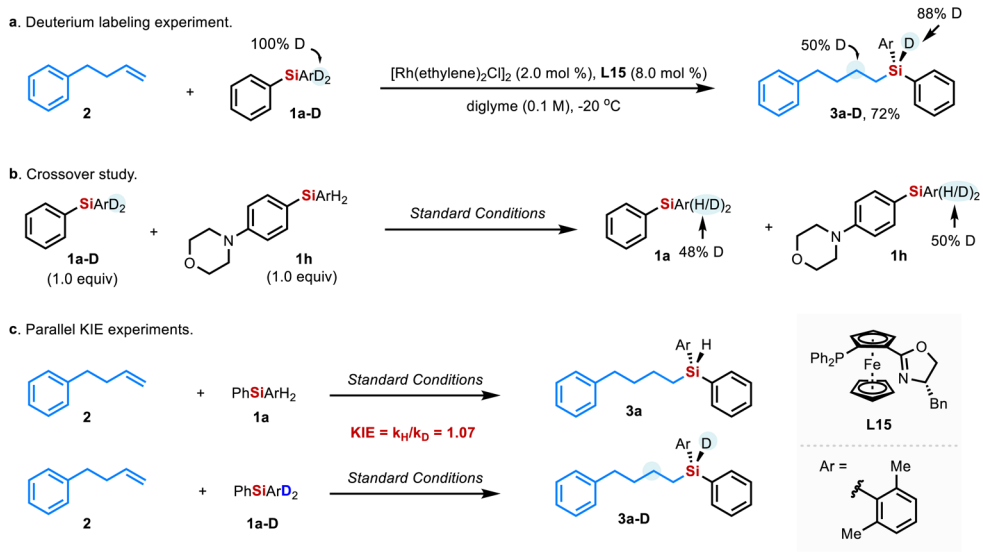

Scheme 6 Mechanistic studies.

deuterium at silicon atom was replaced by hydrogen even using freshly distilled diglyme (for more details, see ESI†). To investigate this further, the reaction between **1a** and **2** was carried out under the same conditions in the presence of 5.0 equivalent of D_2O. The resulting product showed a similar distribution of deuterium despite of the use of undeuterated dihydrosilane **2**, clearly suggesting that the observed deuterium loss in the deuterium labeling experiment might account for trace amount of water in the diglyme. Next, a crossover study was conducted by mixing **1a-D** with **1h** under standard conditions (Scheme 6b), resulting in 48% deuterium remained in **1a** and 50% deuterium transferred to **1h**. The hydrogen–deuterium exchange in crossover experiments indicated reversible Si–H bond activation in the presence of Rh catalyst. In addition, the parallel KIE experiments

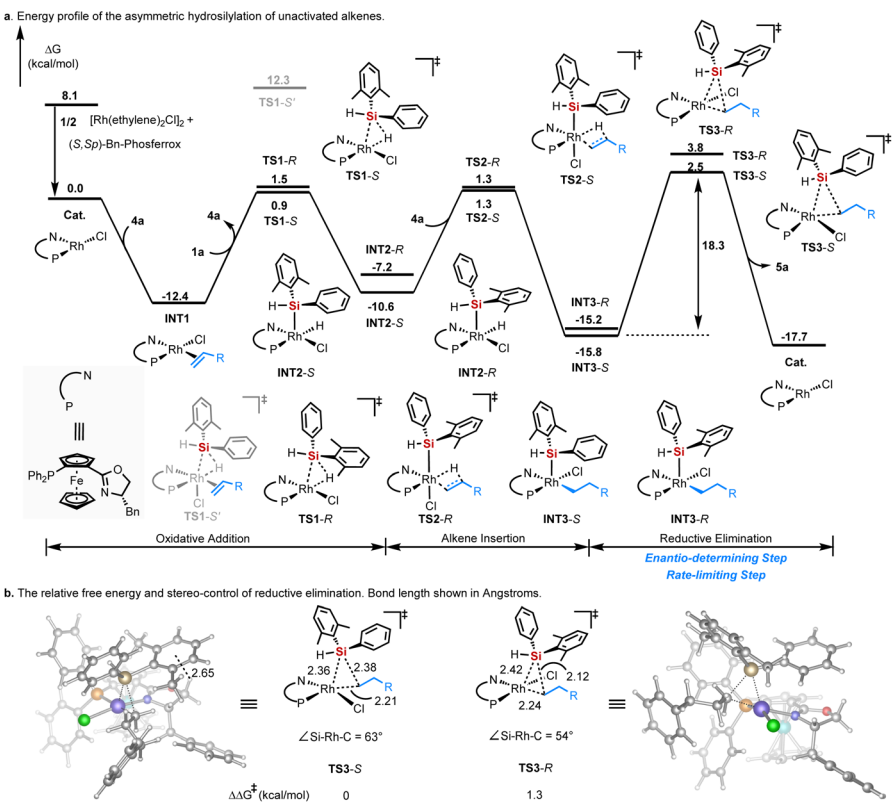

Fig. 1 Energy profile of the asymmetric hydrosilylation of unactivated alkenes.

Open Access Article. Published on 05 June 2025. Downloaded on 2/8/2026 8:22:49 PM. This article is licensed under a Creative Commons Attribution-NonCommercial 3.0 Unported Licence.

were then performed under extremely dried conditions, the KIE value ($k_H/K_D = 1.07$) revealed that the oxidative addition of Si–H bond is not involved in the rate-determining step of this reaction (Scheme 6c), which is consistent with our mechanistic hypothesis.

To further understand the mechanism and disclose the stereocontrol origin of this Rh-catalysed asymmetric hydrosilylation, density functional theory (DFT) calculations using Gaussian 09 software were carried out based on the ωB97XD/6-31G(d,p)/Lanl2TZ(Rh)/def2-SVP(Fe) level of theory. As shown in Fig. 1, it is an exothermic process (8.1 kcal mol^{-1}) to form the catalytic species **Cat.** by the ligand exchange between the $[Rh(ethylene)_2Cl]_2$ and chiral ligand (*S*,*Sp*)-Bn-phosferrox. The following reaction pathway initiated by **Cat.** were involved Si–H oxidative addition, alkene insertion, and reductive elimination to release **5a**. The overall energy profile tends to be relatively low activation barrier for each step and regenerate the **Cat.** for the next catalytic cycle, suggesting this hydrosilylation would be rather reactive consistent with the low reaction temperature. The oxidative addition of Si–H bond with Rh(I) metal *via* its d_{z^2} orbital have to dissociate alkene coordination to enhance its oxidation ability (the unfavorable **TS1**-*S*′, see ESI Table S7† for details), displaying a reversible barrier *via* **TS1**-*S*/**TS1**-*R*, which are consistent with the crossover study and parallel KIE experiments in Scheme 6b and c. The high regio-selective step of alkene insertion to Rh–H bond (Chalk–Harrod mechanism) is the low barrier and reversible, although the quite similar energy of transition states cannot differentiate well for enantio-control (Fig. S13†). Both the enantio-determining and rate-limiting step was predicted to be the reductive elimination step for the formation of C–Si bond *via* **TS3**-*S* or **TS3**-*R* of **INT3**-*S*. More inspections of the C–Si bond reductive elimination, different coordinated scenarios had been proposed to evaluate the final stereo-control, involving the forming C–Si bond *trans*-position to N or P coordination of chiral ligand (see ESI Fig. S15† for details). The *S*-isomer control seems to undergo a favorable trans effect, and the Rh–C bond at the *trans*-position of P coordination is activated, supporting by the corresponding intermediate in Fig. S14.† Compared with **TS3**-*R*, **TS3**-*S* has shorter Rh–Si/Rh–C bonds and longer C–Si bond, the character of early transition state facilitated this enantio-determined reductive elimination for *S*-isomer. In considering the more possible conformations of transition states in ESI,† the *S*-isomer on silicane center dominated the calculated structures, which stabilize by the C–H–π interaction between the oxazoline and arene substituent of silicane group, leading to *S*-configuration for **5a** product. And the predicted enantioselectivity would be 81% ee based on the Boltzmann distribution, which are in agreement with the experimental 87% ee in Scheme 4. These findings further reinforce the hypothesis that desymmetrization of the dihydrosilane is crucial in determining the stereochemical outcome.

Conclusions

In summary, we have demonstrated a rhodium-catalysed enantioselective hydrosilylation of unactivated alkenes, enabling the efficient construction of Si-stereogenic silanes with excellent regioselectivity and high enantioselectivity. This reaction features a broad substrate scope, and excellent functional group and heterocycle compatibility including traditionally challenging strong coordinating groups. The successful application of this method in late-stage functionalization of bioactive compounds and the synthesis of a bioactive analogue underscore its potential utility in medicinal chemistry, particularly for the development of silicon-containing pharmaceuticals. Ongoing studies in our laboratory focus on further expanding the scope of Si-stereogenic derivatives *via* catalytic asymmetric hydrosilylation.

Date availability

Further details of the experimental procedure, X-ray crystallographic data, ^1H, ^{13}C, ^{19}F and ^{29}Si NMR spectra, HPLC charts, and computational details are available in the ESI.†

Author contributions

P. W. conceived the concept and directed the project. Y. W. and H.-Y. Q. conducted the experiments and developed the reactions. Q.-Y. W., X.-X. N., L. Z. assisted with some substrate preparation and data analysis. H. Z., J.-Y. Z. and Q. P. performed the computational calculations. Y. W., Q. P. and P. W. co-wrote the manuscript. All authors contributed to discussion.

Conflicts of interest

There are no conflicts to declare.

Acknowledgements

We gratefully acknowledge National Key R&D Program of China (2023YFF0723900), National Natural Science Foundation of China (22371293, 92156017, 22171277, 22101291), Strategic Priority Research Program of the Chinese Academy of Sciences (XDB1180000), Program of Shanghai Academic/Technology Research Leader (23XD1424500), "Frontiers Science Center for New Organic Matter", Nankai University (No. 63181206) and Haihe Laboratory of Sustainable Chemical Transformation of Tianjin (No. 24HHWCSS00019), Shanghai Institute of Organic Chemistry (SIOC), and State Key Laboratory of Organometallic Chemistry for financial support. We also thank Y.-C. Li at SIOC for verifying the reproducibility of this work.

Notes and references

1 (*a*) R. Tacke and H. Linoh, in *Organic Silicon Compound*, Wiley-VCH, 1989, pp. 1143–1206; (*b*) M.-L. Abel, in *Handbook of Adhesion Technology*, ed. L. F. M. da Silva, A. Öchsner and R. D. Adams, Springer International Publishing, Cham, 2018, pp. 257–280; (*c*) *Organosilicon Chemistry: Novel Approaches and Reactions*, ed. T. Hiyama and M. Oestreich, Wiley-VCH Verlag GmbH & Co. KGaA., 2019; (*d*) M. A. Brook, *Silicon in Organic, Organometallic,*

© 2025 The Author(s). Published by the Royal Society of Chemistry

Open Access Article. Published on 05 June 2025. Downloaded on 2/8/2026 8:22:49 PM. This article is licensed under a Creative Commons Attribution-NonCommercial 3.0 Unported Licence.

and Polymer Chemistry, J. Wiley and Sons, New York, 2000; (*e*) J. Y. Corey, in *Adv. Organomet. Chem.*, ed. A. F. Hill and M. J. Fink, Academic Press, 2011, vol. 59, pp. 181–328.

2 (*a*) V. L. H. Sommer, *Stereochemistry, Mechanism and Silicon*, McGraw-Hill Book Comp., 1965; (*b*) R. J. P. Corriu, C. Guérin and J. J. E. Moreau, in *Topics in Stereochemistry*, 1984, pp. 43–198; (*c*) K. Igawa and K. Tomooka, Chiral Silicon Molecules, in *Organosilicon Chemistry*, Wiley-VCH, 2019, pp. 495–532; (*d*) T. H. Chan and D. Wang, *Chem. Rev.*, 1992, **92**, 995–1006; (*e*) M. Oestreich, *Synlett*, 2007, **2007**, 1629–1643; (*f*) G. Luo, L. Chen, Y. Li, Y. Fan, D. Wang, Y. Yang, L. Gao, R. Jiang and Z. Song, *Org. Chem. Front.*, 2021, **8**, 5941–5947; (*g*) J. Zhu, S. Chen and C. He, *J. Am. Chem. Soc.*, 2021, **143**, 5301–5307; (*h*) B. Yang, J. Gao, X. Tan, Y. Ge and C. He, *Angew. Chem., Int. Ed.*, 2023, **62**, e202307812.

3 (*a*) M. Oestreich, *Chem.–Eur. J.*, 2006, **12**, 30–37; (*b*) A. Weickgenannt, M. Mewald and M. Oestreich, *Org. Biomol. Chem.*, 2010, **8**, 1497–1504.

4 (*a*) X. Chang, P.-L. Ma, H.-C. Chen, C.-Y. Li and P. Wang, *Angew. Chem., Int. Ed.*, 2020, **59**, 8937–8940; (*b*) H. Zhang and D. Zhao, *ACS Catal.*, 2021, **11**, 10748–10753; (*c*) T. Liu, X.-R. Mao, S. Song, Z.-Y. Chen, Y. Wu, L.-P. Xu and P. Wang, *Angew. Chem., Int. Ed.*, 2023, **62**, e202216878; (*d*) H. Li, P.-G. Zhao, C.-Y. Wang, R.-Y. Zhang, J.-J. Li, Y. Wu and P. Wang, *Org. Lett.*, 2023, **25**, 3859–3863; (*e*) Z.-D. Li, F. Ren, Y. Wu, J.-J. Li, J. Luo and P. Wang, *Org. Lett.*, 2024, **26**, 7436–7441.

5 (*a*) L.-W. Xu, L. Li, G.-Q. Lai and J.-X. Jiang, *Chem. Soc. Rev.*, 2011, **40**, 1777–1790; (*b*) R. Shintani, *Asian J. Org. Chem.*, 2015, **4**, 510–514; (*c*) J. O. Bauer and C. Strohmann, *Eur. J. Inorg. Chem.*, 2016, **2016**, 2868–2881; (*d*) R. Shintani, *Synlett*, 2018, **29**, 388–396; (*e*) L. Zheng, X.-X. Nie, Y. Wu and P. Wang, *Eur. J. Org Chem.*, 2021, **2021**, 6006–6014; (*f*) Y. Wu and P. Wang, *Angew. Chem., Int. Ed.*, 2022, **61**, e202205382; (*g*) W. Yuan and C. He, *Synthesis*, 2022, **54**, 1939–1950; (*h*) Y. Ge, X. Huang, J. Ke and C. He, *Chem Catal.*, 2022, **2**, 2898–2928; (*i*) Y. Wu, L. Zheng, Y. Wang and P. Wang, *Chem*, 2023, **9**, 3461–3514; (*j*) J. Zhao, Y. Ge and C. He, *Chin. J. Org. Chem.*, 2023, **43**, 3352–3366; (*k*) F. Y. Yan Zeng, *Chin. J. Org. Chem.*, 2023, **43**, 3388–3413; (*l*) L. Li, W.-S. Huang, Z. Xu and L.-W. Xu, *Sci. China: Chem.*, 2023, **66**, 1654–1687; (*m*) Z.-T. Ye, Z.-W. Wu, X.-X. Zhang, J. Zhou and J.-S. Yu, *Chem. Soc. Rev.*, 2024, **53**, 8546–8562; (*n*) Y. Ge, J. Ke and C. He, *Acc. Chem. Res.*, 2025, **58**, 375–398.

6 Selected examples on catalytic hydrosilylation of alkenes, see:(*a*) K. Tamao, K. Nakamura, H. Ishii, S. Yamaguchi and M. Shiro, *J. Am. Chem. Soc.*, 1996, **118**, 12469–12470; (*b*) Y. Naganawa, T. Namba, M. Kawagishi and H. Nishiyama, *Chem.–Eur. J.*, 2015, **21**, 9319–9322; (*c*) G. Zhan, H.-L. Teng, Y. Luo, S.-J. Lou, M. Nishiura and Z. Hou, *Angew. Chem., Int. Ed.*, 2018, **57**, 12342–12346; (*d*) T. He, L.-C. Liu, W.-P. Ma, B. Li, Q.-W. Zhang and W. He, *Chem.–Eur. J.*, 2020, **26**, 17011–17015; (*e*) Y.-H. Huang, Y. Wu, Z. Zhu, S. Zheng, Z. Ye, Q. Peng and P. Wang, *Angew. Chem., Int. Ed.*, 2022, **61**, e202113052; (*f*) W. Lu, Y. Zhao and F. Meng, *J. Am. Chem. Soc.*, 2022, **144**, 5233–5240; (*g*) L. Wang, W. Lu, J. Zhang, Q. Chong and F. Meng, *Angew. Chem., Int. Ed.*, 2022, **61**, e202205624; (*h*) F.-H. Gou, F. Ren, Y. Wu and P. Wang, *Angew. Chem., Int. Ed.*, 2024, **63**, e202404732; (*i*) B. Fu, L. Wang, K. Chen, X. Yuan, J. Yin, S. Wang, D. Shi, B. Zhu, W. Guan, Q. Zhang and T. Xiong, *Angew. Chem., Int. Ed.*, 2024, **63**, e202407391; (*j*) L. Wu, L. Zhang, J. Guo, J. Gao, Y. Ding, J. Ke and C. He, *Angew. Chem., Int. Ed.*, 2024, **63**, e202413753.

7 Catalytic hydrosilylation of alkynes, see:(*a*) K. Igawa, D. Yoshihiro, N. Ichikawa, N. Kokan and K. Tomooka, *Angew. Chem., Int. Ed.*, 2012, **51**, 12745–12748; (*b*) R.-H. Tang, Z. Xu, Y.-X. Nie, X.-Q. Xiao, K.-F. Yang, J.-L. Xie, B. Guo, G.-W. Yin, X.-M. Yang and L.-W. Xu, *iScience*, 2020, **23**, 101268; (*c*) J.-L. Xie, Z. Xu, H.-Q. Zhou, Y.-X. Nie, J. Cao, G.-W. Yin, J.-P. Bouillon and L.-W. Xu, *Sci. China: Chem.*, 2021, **64**, 761–769; (*d*) Y. Zeng, X.-J. Fang, R.-H. Tang, J.-Y. Xie, F.-J. Zhang, Z. Xu, Y.-X. Nie and L.-W. Xu, *Angew. Chem., Int. Ed.*, 2022, **61**, e202214147; (*e*) F.-Y. Ling, F. Ye, X.-J. Fang, X.-H. Zhou, W.-S. Huang, Z. Xu and L.-W. Xu, *Chem. Sci.*, 2023, **14**, 1123–1131; (*f*) H. Wen, X. Wan and Z. Huang, *Angew. Chem., Int. Ed.*, 2018, **57**, 6319–6323.

8 Catalytic hydrosilylation of carbonyl compounds, see:(*a*) T. Hayashi, K. Yamamoto and M. Kumada, *Tetrahedron Lett.*, 1974, **15**, 331–334; (*b*) R. J. P. Corriu and J. J. E. Moreau, *J. Organomet. Chem.*, 1974, **64**, C51–C54; (*c*) R. J. P. Corriu and J. J. E. Moreau, *J. Organomet. Chem.*, 1975, **85**, 19–33; (*d*) T. Ohta, M. Ito, A. Tsuneto and H. Takaya, *J. Chem. Soc., Chem. Commun.*, 1994, **1994**, 2525–2526; (*e*) Y. Ding, J. Ke, W. Zhang, B. Li and C. He, *Chem. Commun.*, 2024, **60**, 13734–13737.

9 (*a*) Y. Kuninobu, K. Yamauchi, N. Tamura, T. Seiki and K. Takai, *Angew. Chem., Int. Ed.*, 2013, **52**, 1520–1522; (*b*) M. Murai, H. Takeshima, H. Morita, Y. Kuninobu and K. Takai, *J. Org. Chem.*, 2015, **80**, 5407–5414; (*c*) B. Yang, W. Yang, Y. Guo, L. You and C. He, *Angew. Chem., Int. Ed.*, 2020, **59**, 22217–22222; (*d*) W. Ma, L.-C. Liu, K. An, T. He and W. He, *Angew. Chem., Int. Ed.*, 2021, **60**, 4245–4251; (*e*) S. Chen, D. Mu, P. L. Mai, J. Ke, Y. Li and C. He, *Nat. Commun.*, 2021, **12**, 1249; (*f*) Y. Guo, M.-M. Liu, X. Zhu, L. Zhu and C. He, *Angew. Chem., Int. Ed.*, 2021, **60**, 13887–13891; (*g*) S. Chen, J. Zhu, J. Ke, Y. Li and C. He, *Angew. Chem., Int. Ed.*, 2022, **61**, e202117820.

10 (*a*) Y. Yasutomi, H. Suematsu and T. Katsuki, *J. Am. Chem. Soc.*, 2010, **132**, 4510–4511; (*b*) Y. Nakagawa, S. Chanthamath, I. Fujisawa, K. Shibatomi and S. Iwasa, *Chem. Commun.*, 2017, **53**, 3753–3756; (*c*) J. R. Jagannathan, J. C. Fettinger, J. T. Shaw and A. K. Franz, *J. Am. Chem. Soc.*, 2020, **142**, 11674–11679.

11 (*a*) Y. Kurihara, M. Nishikawa, Y. Yamanoi and H. Nishihara, *Chem. Commun.*, 2012, **48**, 11564–11566; (*b*) L. Chen, J.-B. Huang, Z. Xu, Z.-J. Zheng, K.-F. Yang, Y.-M. Cui, J. Cao and L.-W. Xu, *RSC Adv.*, 2016, **6**, 67113–67117; (*c*) R. Shintani, H. Otomo, K. Ota and T. Hayashi, *J. Am. Chem. Soc.*, 2012, **134**, 7305–7308; (*d*) Z.-Z. Zhao, X. Pang, X.-X. Wei, X.-Y. Liu and X.-Z. Shu, *Angew. Chem., Int. Ed.*, 2022, **61**, e202200215.

12 For selected books and reviews, see:(*a*) *Comprehensive Handbook on Hydrosilylation*, ed. B. Marciniec, Pergamon,

Open Access Article. Published on 05 June 2025. Downloaded on 2/8/2026 8:22:49 PM.
This article is licensed under a Creative Commons Attribution-NonCommercial 3.0 Unported Licence.

1992; (*b*) J. Tang and T. Hayashi, Asymmetric Hydrosilylation, in *Catalytic Heterofunctionalization*, ed. A. Togni and H. Grutzmacher, Wiley-VCH, 2001, pp. 73–90; (*c*) T. Hayashi and K. Yamasaki, C–E Bond Formation through Asymmetric Hydrosilylation of Alkenes, *Comprehensive Organometallic Chemistry III*, ed. R. H. Crabtree and D. M. P. Mingos, Elsevier, 2007; (*d*) B. Marciniec, *Hydrosilylation: A Comprehensive Review on Recent Advances*, Springer, 2009, vol. 1, Part 1; (*e*) J. Guo, Z. Cheng, J. Chen, X. Chen and Z. Lu, *Acc. Chem. Res.*, 2021, **54**, 2701–2716.

13 During the submission of this manuscript, a copper-catalysed asymmetric hydrosilylation of alkenes has been reported, see: X.-Y. Zhu, W. Gao, J.-L. Xu, Z.-L. Wang, J.-B. Zhao and Y.-H. Xu, *Nat. Commun.*, 2025, **16**, 378. Also see our pre-print uploaded on Oct. 29, 2024, Chemrxiv, 2024, DOI: 10.26434/chemrxiv-2024-3tlq2.

14 Deposition number 2393477 (5j) contain the supplementary crystallographic data for this paper. These data are provided free of charge by the joint Cambridge Crystallographic Data Centre and Fachinformationszentrum Karlsruhe Access Structures service.

© 2025 The Author(s). Published by the Royal Society of Chemistry